Building Height Estimation from Open Optical Remote Sensing by Machine Learning Regression Technique: A Case Study of the Central of Bangkok

Srinoi, T., Bannakulpiphat, T., Santitamnont, P.* and Vaiphasa, C.
Mapping and Positioning from Space (MAPS) Technology Research Center, Department of Survey Engineering, Faculty of Engineering, Chulalongkorn University, Thailand
E-mail: thepchaisrinoi@gmail.com, thirawat.bannakulpiphat@gmail.com, phisan.chula@gmail.com*
chaichoke.v@chula.ac.th
**Corresponding Author*

DOI: https://doi.org/10.52939/ijg.v20i9.3543

Abstract
*Building height is crucial for understanding the urban environment and human activity. In Bangkok, there is open building footprint polygon layer, but it still lacks building height data. Recently, a digital surface model (DSM) from an unmanned aerial vehicle (UAV) was obtained for referencing. Additionally, open medium-resolution optical satellite images are freely provided almost a decade. Both data sources were used in research to estimate building heights. The study demonstrated that optical remote sensing, combined with reference height data, can effectively estimate building heights in urban areas. In this research we deploy two approaches namely, support vector machine regression (SVR) and random forest regression (RFR). The result produced similar root mean square error (RMSE) values: approximately **6.6** meters for buildings under 50 meters and around 12 meters for buildings under 100 meters. However, when evaluated with the **50**-meter building height group in the second model testing, the SVR algorithm performed better than the RFR algorithm.*

Keywords: Machine Learning, Optical Remote Sensing, Regression, Urban Height Estimation

1. Introduction

Urban areas are regions where a dense population resides within a specific space. Approximately three-quarters of the global population currently reside in urban areas [1]. Unlike rural areas, where agriculture is the primary occupation, urban residents typically engage in a variety of non-agricultural professions. The primary function of urban areas is to serve as commercial hubs. Additionally, urban centers often have specialized roles, including administration, transportation, public health, and education. People from rural areas often seek to improve their quality of life by moving to cities for better job opportunities and living conditions. These functions act as pull factors for urban migration, consistent with Lee's migration model. Urban land, especially in central business districts, is very expensive. To maximize the use of this limited space, high-rise buildings are constructed, allowing many people to live and work within a small area. Therefore, the identity of urban areas is defined by their numerous and diverse tall buildings. The prevalence of these tall structures contributes to urban pollution and urban heat island phenomenon [2].

Building footprint and height data are crucial components of town planning and administration in any country, as they provide valuable insights into population density distribution [3], energy consumption [4], and patterns of human activity. Currently, open building footprint data are available from sources such as Microsoft Global Building Footprint [5] and Google Open Buildings [6]. These datasets are derived from high-resolution satellite imagery using image segmentation and deep learning techniques. However, open building height data remains unavailable. Recently, research papers have focused on estimating building heights using open remote sensing data. Satellite images and sample height data are used as the feature input and output of regression models, respectively. Firstly, a continental-scale building height estimation model was developed and studied in various states across the United States using RADAR satellite imagery [7].

This model was further extended to the northern continental zone, including the USA, Europe, and China, employing the Random Forest Regressor method with both RADAR and optical satellite imagery [8]. Subsequently, research focused on height estimation at a medium spatial resolution of ten meters in Germany using support vector machine regression [9], and in China using random forest regression [10]. These efforts produced estimation raster grids that achieved height estimation errors at the meter scale. In Bangkok, the capital of Thailand, the Bangkok Metropolitan Electrical Authority (MEA) conducted a surveying project utilizing an unmanned aerial vehicle (UAV) equipped with an oblique camera. This UAV with an inclined views captured building shapes over area about 10-square kilometer in the central business district of Bangkok, producing various photogrammetric products including digital surface models (DSMs) and mesh of the building model as shown in Figure 1 [11]. These DSMs were used to measure building heights, incorporating building footprint data from Microsoft. Optical satellite imagery can now be easily downloaded from Google Earth Engine, providing access to images like LANDSAT 8 and SENTINEL-2 across multiple years.

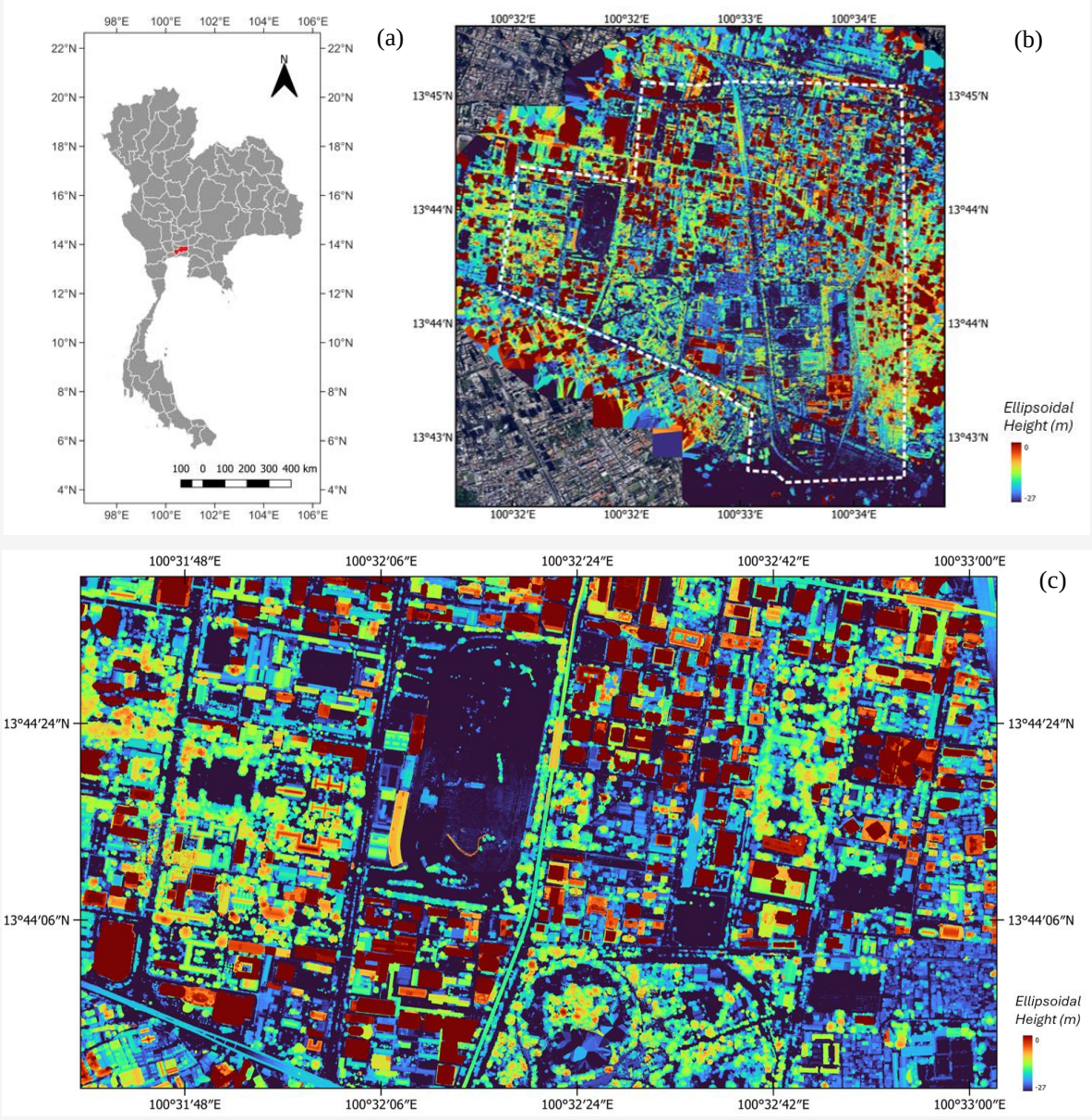

Figure 1: Digital surface model of the study area
(a) Bangkok, Thailand (b) UAV-DSM of Bangkok urban area (c) UAV-DSM in specific area

These images can be filtered by parameters such as cloud cover and area coverage, which is crucial for image preparation in Thailand's tropical climate, where clouds and rain are frequent. Individual building heights can be derived from DSMs. By comparing the estimated raster grid output with the DSMs, we can assess accuracy and improvements. This presents a promising opportunity for utilizing open digital surface models in future research. Consequently, building height estimation research has been successfully conducted in the Bangkok urban area.

This study aims to produce building height estimations for the Bangkok urban area using open optical satellite images and popular machine learning regression models such as support vector machine regression and random forest regression, as used in previous research. Furthermore, we aim to compare the normalized digital surface model (nDSM) from UAV data with height estimation models derived from open optical remote sensing using different techniques. This research is essential for demonstrating the potential of optical satellite imagery in urban height estimation, which will lay the groundwork for future studies on land cover height or DSM estimation.

2. Data Description

2.1 Optical Satellite Imagery

Various sources provide feature inputs for analysis, one of which is optical satellite imagery, also known as visible-near infrared satellite imagery. Sensors on Earth observation satellites detect the spectral reflectance of the Earth's surface and convert this data into digital numbers stored in images. Reflectance values at different wavelengths are stored separately in raster bands, with the spectral resolution indicating the number of bands captured by the sensor. Since Earth's surface data changes over time, multitemporal satellite images allow us to monitor land cover changes. These satellites collect data repeatedly based on their temporal resolution. Currently, medium spatial resolution satellite images, which indicate the smallest detectable objects about more than 10 meters, can be freely downloaded from the internet. Sentinel-2 Surface Reflectance imagery for a small urban area in Bangkok was analyzed and processed using the Google Earth Engine service.

Six cloud-free images from 2022 were manually selected on the following dates: January 1st, April 16th, June 20th, October 18th, November 2nd, and December 12th. Specific bands (B2, B3, B4, B5, B6, B7, B8, B8A, B11, and B12) were chosen. The description of these bands [12] is illustrated in Table 1. Subsequently, indices such as the Normalized Difference Vegetation Index (NDVI), Modified Normalized Difference Water Index (MNDWI), and Normalized Difference Built-up Index (NDBI) were opted and calculated using Equations 1, 2 and 3.

$$NDVI = \frac{\rho_{NIR} - \rho_{RED}}{\rho_{NIR} + \rho_{RED}} \quad \text{Equation 1}$$

$$MDNWI = \frac{\rho_{GREEN} - \rho_{SWIR}}{\rho_{GREEN} + \rho_{SWIR}} \quad \text{Equation 2}$$

$$NDBI = \frac{\rho_{SWIR} - \rho_{NIR}}{\rho_{SWIR} + \rho_{NIR}} \quad \text{Equation 3}$$

Where ρ_{GREEN}, ρ_{RED}, and ρ_{NIR} are the digital number values from the satellite image corresponding to the green (B3), red (B4), near infrared (B8) and short-wave infrared (B11) bands, respectively.

The earlier study [10] indicated that the backscatter coefficient from RADAR remote sensing and the shading index that linked to infrared bands from optical remote sensing are the most essential variables in building height estimation models. The shadows of tall buildings change seasonally due to the sun's altitude, which contributes to the sun's declination as shown in Figure 2. Optical imagery products significantly outperform RADAR imagery products. For example, Sentinel-1 provides only VV and VH polarization data, whereas PALSAR-2 offers HH and HV polarization data at higher spatial resolution. The VVH index might be calculated to enhance model predictions [7] and [10]. RADAR imagery typically offers only five bands, whereas optical imagery provides around ten bands, as shown in Table 1, allowing for a wider selection of bands. Research conducted in Berlin [9] demonstrated that the Optical Only model resulted in a height estimation error of less than 50 cm, which was lower than that of the RADAR Only model. Therefore, this study will consider only optical remote sensing for this new area of research.

2.2 Building Footprint and Heigh

A building footprint is a polygon that represents the ground coverage of a building, distinct from the roofline, which can be delineated directly from a distorted geospatial image. Building height can be measured using various methods, including trigonometric leveling, photogrammetric intersection, laser scanning, shadow measurement, and digital elevation models (DEMs).

Table 1: Description of Sentinel-2 Satellite bands used in this research

Band no.	Spatial Resolution (m)	Wavelength (Name of Satellite System)	Description
B2	10 m	496.6nm (S2A) / 492.1nm (S2B)	Blue
B3	10 m	560nm (S2A) / 559nm (S2B)	Green
B4	10 m	664.5nm (S2A) / 665nm (S2B)	Red
B5	20 m*	703.9nm (S2A) / 703.8nm (S2B)	Red Edge 1
B6	20 m*	740.2nm (S2A) / 739.1nm (S2B)	Red Edge 2
B7	20 m*	782.5nm (S2A) / 779.7nm (S2B)	Red Edge 3
B8	10 m	835.1nm (S2A) / 833nm (S2B)	Near Infrared
B8A	20 m*	864.8nm (S2A) / 864nm (S2B)	Red Edge 4
B11	20 m*	1613.7nm (S2A) / 1610.4nm (S2B)	Short Wave Infrared 1
B12	20 m*	2202.4nm (S2A) / 2185.7nm (S2B)	Short Wave Infrared 2

Figure 2: Sentinel-2 Imagery at different time of the year captured from google earth engine in python (google colab) version (a) summer solstices June 20th, 2022 (b) near winter solstices December 12th, 2022

These height measurements can be integrated into the attribute table of a building layer, enabling the visualization of simple three-dimensional maps with extruded polygons. This study utilized a digital surface model (DSM) derived from photogrammetric products captured by an oblique camera mounted on an unmanned aerial vehicle. Microsoft Building Footprint data was used as sample building data. This dataset, available for download (https://github.com/phisan-chula/Thai_Bldg_Model) by province in Thailand, comes in GeoPackage and includes both polygon and centroid layers [13].

2.3 Machine Learning Regression Model

The purpose of a regression model is to predict quantitative data. Recently, machine learning algorithms have become popular methods for creating regression models. The process begins with collecting features and output samples. Next, exploratory data analysis or feature engineering is performed. The data is then divided into two groups: the training dataset and the testing dataset. The training dataset is used to develop the model with specific hyperparameters, while the testing dataset, kept separate, is used to evaluate the model by comparing the estimated values to their reference values.

Model performance can be assessed using indicators such as Root Mean Square Error (RMSE), Mean Absolute Error (MAE), Pearson Coefficient (R), and the Coefficient of Determination (R^2). This study used only RMSE and R^2. The equations for both indicators are shown in Equations 4 and 5.

$$RMSE = \sqrt{\frac{\sum_{i=1}^{N}(H_{pred,i} - H_{ref,i})^2}{N}} \quad \text{Equation 4}$$

$$R^2 = \frac{\sum_{i=1}^{N}(H_{pred,i} - \bar{H}_{ref})^2}{\sum_{i=1}^{N}(H_{ref,i} - \bar{H}_{ref})^2} \quad \text{Equation 5}$$

Where in our dataset has two groups with N sample: reference dataset has $H_{ref,1}$, $H_{ref,2}$, …, $H_{ref,N}$ that corresponds to predicted dataset that has $H_{pred,1}$, $H_{pred,2}$, …, $H_{pred,N}$, respectively. And $\bar{H}_{ref}$ is the average of H_{ref}.

In this research, Support Vector Machine Regression (SVR) and Random Forest Regression (RFR) were chosen to develop the building height estimation model. SVR works by calculating the parameters of an n-dimensional hyperplane from n-1 dimensional feature inputs. To enhance performance, kernel functions, such as linear or radial basis functions, are used to map the features to a higher dimension for model creation. RFR, on the other hand, involves generating a group of decision trees. The feature input is sampled for constructing each tree, followed by pruning to reduce overfitting. Each tree provides one estimation output, and the final output is obtained by averaging or taking the majority vote of all the individual tree outputs.

3. Methodologies

The diagram summarizing our research methodologies is shown in Figure 3.

3.1 Feature and Output Data Preparation

For the features of the model, first download the satellite images and calculate the band indices as mentioned earlier. After that, the temporal aggregation was performed using statistical calculations (mean and 10th 25th 50th 75th, and 90th percentiles). Finally, export the feature bands. We now have 10 satellite bands plus 3 indices band, each with 6 statistical calculations, totaling 78 features (13x6). For the output of model, DSM was received from photogrammetric product. Due to limitations of the digital terrain model (DTM) in high-rise building area and because the study area is less than 10 square kilometers, an assumed ground plane at -30 meters ellipsoidal height was selected as DTM to calculate the normalized digital surface model (nDSM), which represents height above the assumed ground level. First, download the building footprint data for Bangkok. Then, sample data from the area and extract raster values from features using median zonal statistics. We assumed that one building floor equals 3 meters [14]. Buildings with heights less than 3 meters or greater than 100 meters were excluded from the dataset. Additionally, buildings with an area coverage of less than 100 square meters (Sentinel-2 pixel resolution) were also removed.

The data was then grouped by building height in one-meter intervals. To address the significant disparity between the number of low-rise and high-rise buildings, we randomly sampled from intervals with fewer than 100 buildings. For further applications, especially for visualizing on a base map, these models require improvement.

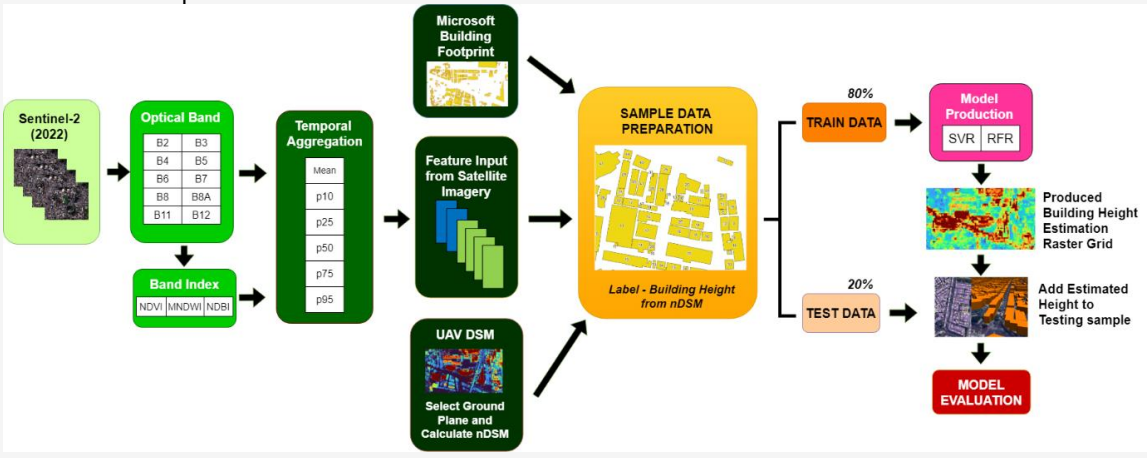

Figure 3: Research methodologies

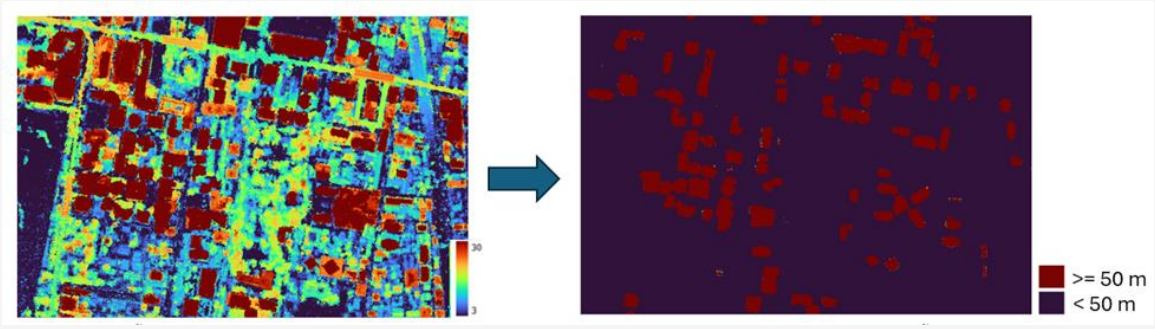

Figure 4: Example of tall building with a height above 50 meters

This is crucial because the Bangkok urban area includes zones with tall buildings exceeding 50 meters, which were excluded from the initial processing, as shown in Figure 4. To address this, we classify building heights into two groups: the first group includes buildings with heights less than 50 meters, while the second group comprises buildings with heights less than 100 meters.

3.2 Model Production and Evaluation

The data was split into training and testing datasets with an 80:20 ratio. The support vector machine regression model was trained using a radial basis function kernel, with the gamma parameter set to 'scale' and the regularization parameter set to 10. Additionally, a random forest regression model was trained separately, utilizing 100 trees, a maximum of 10 features, and the minimum depth parameter set to 'sqrt'. After model training, building height estimation raster grids were generated. The test dataset was then used to obtain predicted heights from the estimation raster using median zonal statistics. Model evaluation was conducted by comparing the predicted heights to the reference heights, calculating the root mean square error (RMSE). A density scatter plot and the coefficient of determination (R^2) were also generated at this stage. For the model evaluation of the second group, we considered the test set that includes both the original data and buildings with heights less than 50 meters. We utilized Python programming with the Scikit-Learn library for model training and evaluation. The hyperparameters were determined through grid search cross-validation on a smaller sample dataset to reduce computational time.

4. Result and Discussion

First, this research focuses on building heights ranging from 3 to 50 meters, as previously studied. The SVR model yielded a root mean square error (RMSE) of 6.6 meters and an R^2 value of 0.40. The RFR model produced an RMSE of 6.7 meters with an R^2 value of 0.33. The difference in RMSE between the two models is approximately 0.1 m, which is negligible given the RMSE scale in meters. Density scatter plots, featuring a unit slope line that depicts the corrected estimation and the linear regression trend of predicted versus reference heights, are shown in Figure 5. However, a limitation of the models is their inability to accurately predict the heights of tall buildings. As illustrated in the figure, the red trend line lies below the white unit slope line at higher reference heights.

Second, we also focused on building heights ranging from 3 to 100 meters. Unlike previous studies, we decided to evaluate two groups: one with heights less than 100 meters and another with heights less than 50 meters. For the SVR model, the RMSE was 12.6 meters with an R^2 value of 0.39 when tested on the less than 100 meters group, and the RMSE was 7.5 meters with an R^2 value of 0.30 when tested on the less than 50 meters group. The RFR model yielded an RMSE of 12.3 meters with an R^2 value of 0.44 for the less than 100 meters group, and an RMSE of 8.6 meters with an R^2 value of 0.08 for the less than 50 meters group. Extending the height interval from less than 50 meters to 100 meters resulted in more than doubling the RMSE. Evaluating the models with the less than 50-meter building height group also led to increased error compared to the initial study, with an additional 1 to 2 meters in RMSE. The RFR model, with an R^2 of 0.08, demonstrated a significantly lower coefficient of determination compared to the support vector machine regression model, which had an R^2 of 0.33.

Additionally, the RMSE from the RFR model was higher than that of the SVR model. Density scatter plots, featuring a unit slope line that depicts the corrected estimation and the linear regression trend of predicted versus reference heights, are also shown in Figure 5. A summary of the model evaluation is shown in Table 2. Figure 6 presents an nDSM from UAV data (reference height) alongside an example of building height estimation raster grids (predicted height), highlighting zones of various building heights.

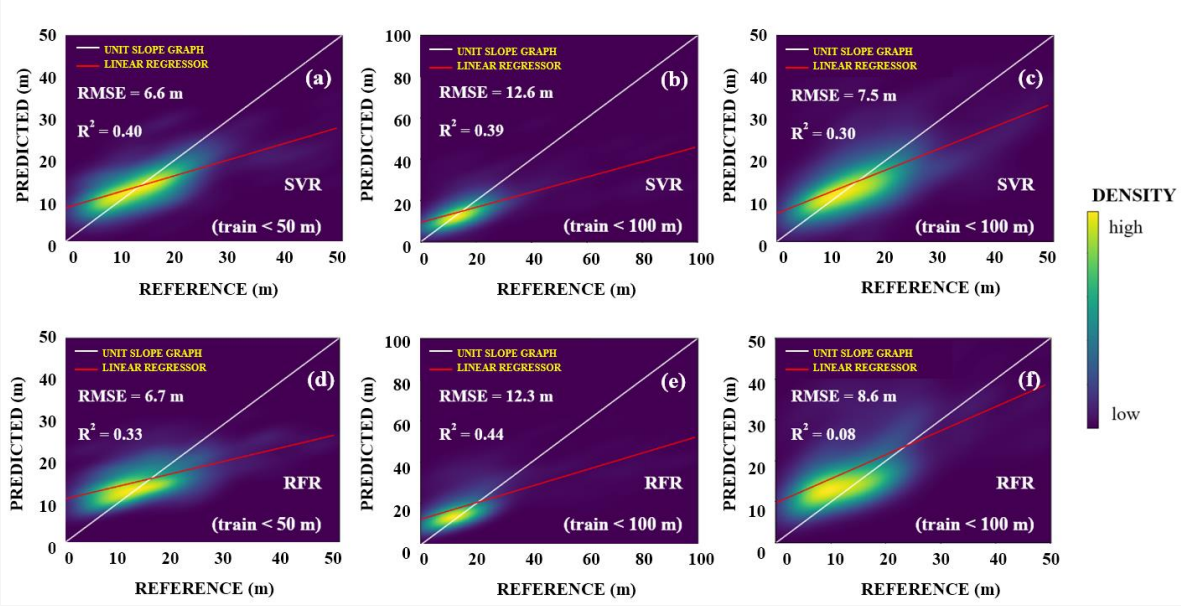

Figure 5: Density scatter plot with linear trend of model evaluation. Results from model trained on the less than 50 m height group: SVR (a) and RFR (d). Results from model trained on the less than 100 m group: tested on the less than 100 m group - SVR (b) and RFR (e); tested on the less than 50 m group - SVR (c) and RFR (f)

Table 2: Model evaluation results

Type	Train: less than 50 m group		Train: less than 100 m group			
	Test: less than 50 m group		Test: less than 100 m group		Test: less than 50 m group	
	RMSE (m)	R^2	RMSE (m)	R^2	RMSE (m)	R^2
SVR	6.6	0.40	12.6	0.39	7.5	0.30
RFR	6.7	0.33	12.3	0.44	8.6	0.08

Additionally, we present the nDSM, resampled to a 10-meter resolution, to visualize alongside the model outputs. These estimations may be influenced by the image's low spatial resolution. Employing different modeling techniques results in varied outputs, as illustrated in Figure 6. The estimation model predicts height on a per-grid basis (pixel-based regression) without considering the spatial context of the image, leading to potentially random visualizations, particularly in the SVR results. Interestingly, the Building Estimation from the SVR Model provided ground height estimates like the reference surface model from UAV data, even though ground height samples were not used for model training. Another example of a larger area was shown in Figure 7. When comparing the SVR results with reference data, we can visualize the height estimation model similarly to a DSM estimation model. However, it is important to note that the model was trained exclusively on building heights, meaning other land cover types were not included in the training process. This limitation should be considered when interpreting the results.

Additionally, we attempted to train models specifically using high-rise buildings, as the previous model, as shown in Figure 5, did not achieve optimal performance with these structures. We collected sample data that exceeded 23 meters [15] to evaluate height estimation models using SVR and RFR. The evaluation results are shown in Figure 8. The SVR model yielded a RMSE of 16.7 meters and an R^2 value of 0.22, while the RFR model produced an RMSE of 16.5 meters with an R^2 value of 0.27. The difference in RMSE between the two models is approximately 0.2 m. This difference in value is small relative to the RMSE values of both models, so this suggests that there are no significant differences between the models.

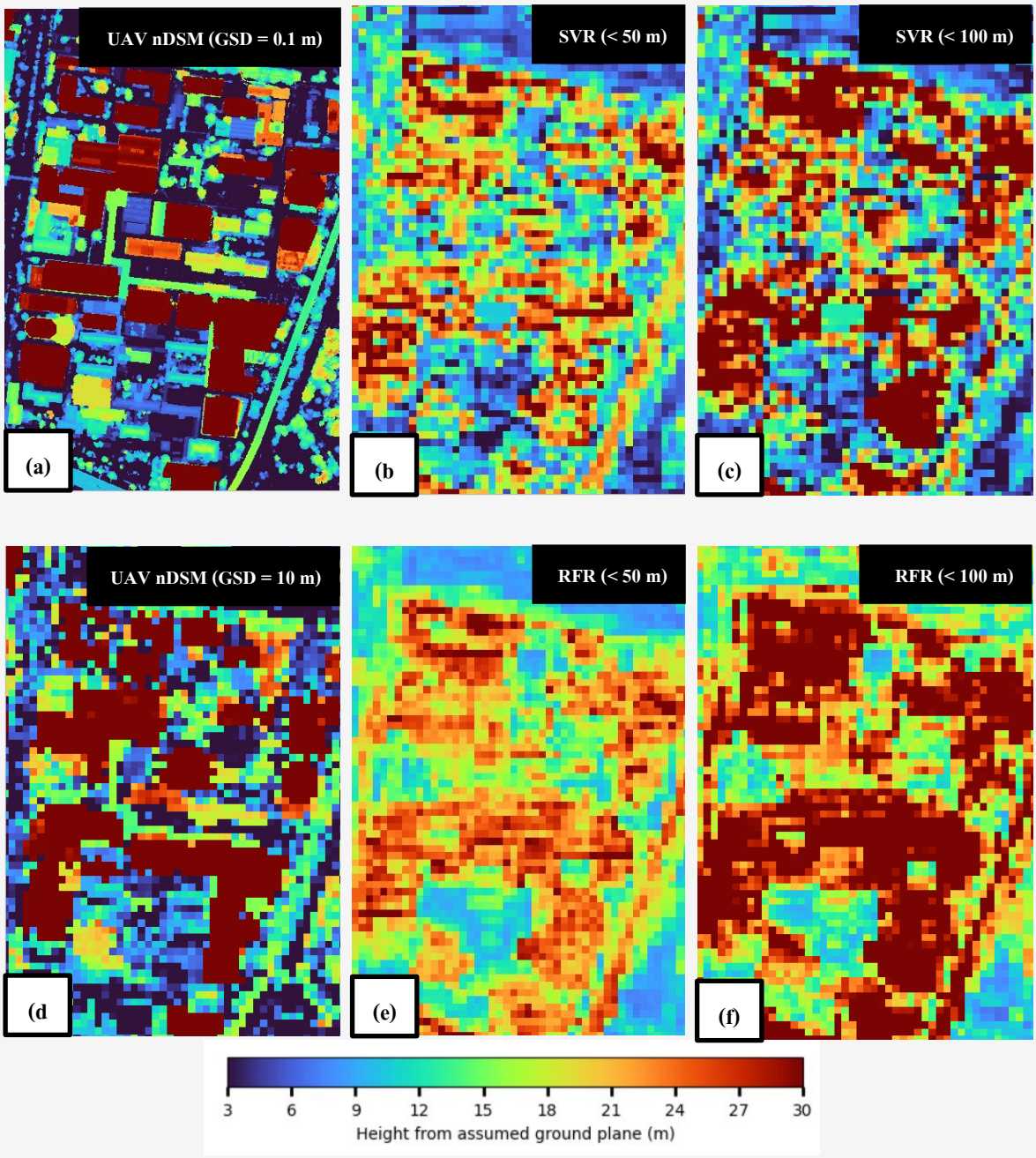

Figure 6: Normalized Digital Surface Model from UAV: Original Version (a) and Resampled Version (d). Building Height Estimation Model Comparison. Results from the model trained on the less than 50 m group: SVR (b) and RFR (e). Results from the model trained on the less than 100 m group: SVR (c) and RFR (f)

Both models exhibit a similar pattern in the density scatter plot, as seen in Figure 8, with overestimation for lower heights and underestimation for higher heights. This issue was interesting to research later that how we combine specific high rise building model to lower building height model. We chose to apply machine learning for building height estimation due to the lack of direct scientific knowledge or established methods for calculating building heights from optical reflectance data. In conclusion, we suggest that this research methodology is well-suited for estimating building heights in urban zones with low- to medium-rise structures, as well as in suburban areas.

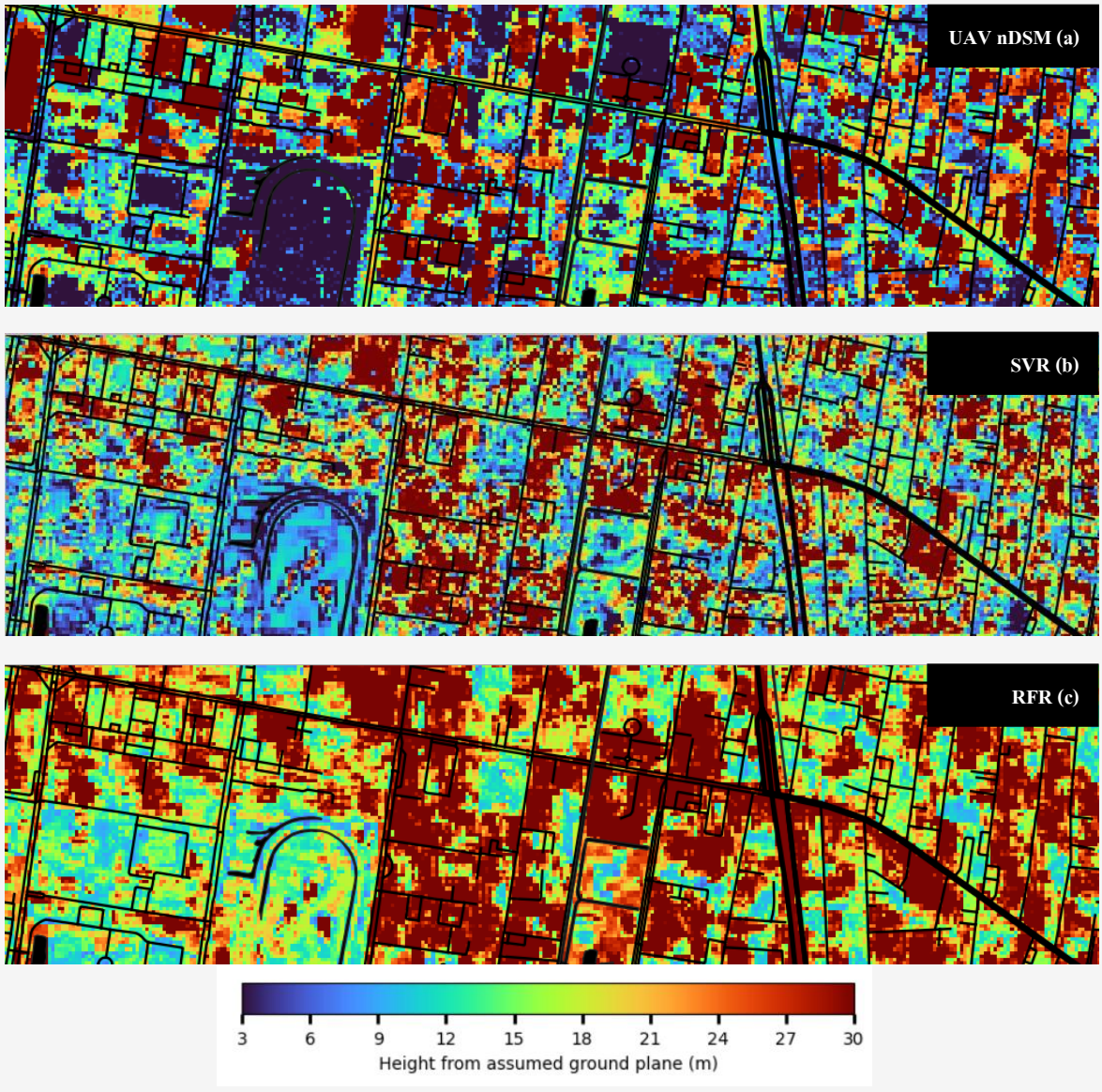

Figure 7: Normalized Digital Surface Model from UAV: Resampled version (a) Estimation results from the model trained on the less than 100 m group: SVR (b) and RFR (c) masked by road and waterbody layer

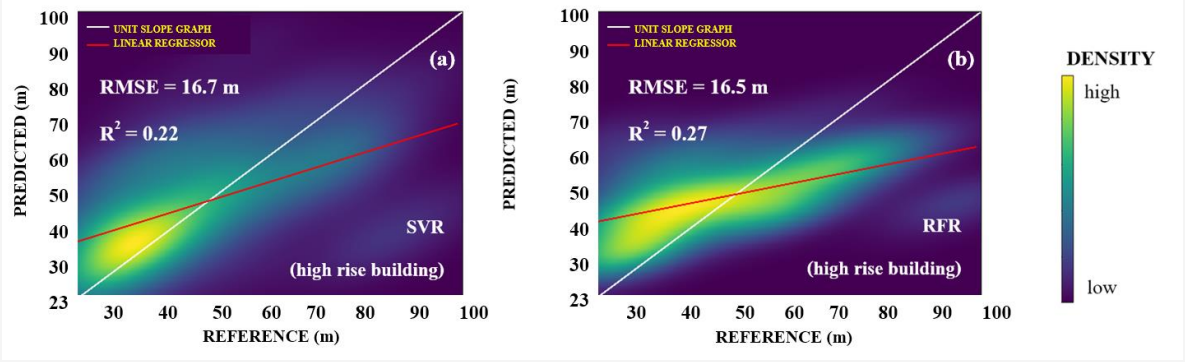

Figure 8: Density scatter plot with linear trend of model evaluation. Results from the model trained on the high rise height group (23 – 100 m): SVR (a) and RFR (b)

5. Conclusion

Optical remote sensing can be utilized to estimate building heights in urban areas. Both support vector machine regression (SVR) and random forest regression (RFR) produced similar root mean square error (RMSE) values: approximately 6.6 meters for buildings under 50 meters and around 12 meters for buildings under 100 meters. However, when evaluated with the 50-meter building height group in the second model testing, the SVR algorithm performed better than the RFR algorithm.

This study showed the potential and limitations of building height estimation from optical remote sensing. We examined the results of elevation models generated by different machine learning algorithms for the urban area of Bangkok, specifically focusing on zones with tall buildings. Buildings under 50 meters were insufficient for accurate urban height estimation mapping, leading to the selection of buildings under 100 meters for model training. This extended height interval, however, resulted in higher height estimation errors. Based on our methodology, we cannot determine the best algorithm for height estimation. Instead, we highlight the differences between the two models and the impact of the height interval sample group on the results. To improve model accuracy, it is essential to increase the sample size, particularly with data from taller buildings, using stratified sampling for better data balance. Additionally, image preprocessing and correction should be implemented, a method for algorithm comparison should be designed, adequate time should be dedicated to hyperparameter tuning, and appropriate model indicators should be selected for evaluation. This methodology should be reevaluated in specific contexts, such as uniform building height zones found in contiguous commercial areas along roads in historic towns or restaurant districts. Additionally, the model should be evaluated using building height statistics and categories to accurately identify its limitations.

By far, we can achieve building height estimation with an accuracy of a few meters. Despite the effort required, this process is valuable for supporting city planning and administration. It has the potential to significantly aid in managing urban growth, particularly in cities like Bangkok, where the number of buildings changes by up to 60,000 annually.

Acknowledgements

The authors express their gratitude to the Metropolitan Electricity Authority (MEA) for providing support for the data used in this research. Additionally, we extend our gratitude to the European Space Agency and the European Commission for providing Sentinel-2 imagery. We also thank the Google Research Team for the Google Earth Engine service, which has greatly facilitated our remote sensing research using geospatial programming. Finally, thank you Microsoft Team and Prof. Dr. Santi Pailoplee (mitrearth) for providing the open geospatial layers.

References

[1] Dijkstra, L., Hamilton, E., Lall, S. and Wahba, S., (2020). How Do We Define Cities, Towns, and Rural Areas? [Online]. Available: https://blogs.worldbank.org/en/sustainablecities/how-do-we-define-cities-towns-and-rural-areas. [Accessed Jun. 10, 2024].

[2] Perini, K. and Magliocco, A., (2014). Effects of Vegetation, Urban Density, Building Height, and Atmospheric Conditions on Local Temperatures and Thermal Comfort. *Urban Forestry and Urban Greening*, Vol. 13, 495–506. https://doi.org/10.1016/j.ufug.2014.03.003.

[3] Alahmadi, M., Atkinson, P. and Martin, D., (2013). Estimating the Spatial Distribution of the Population of Riyadh, Saudi Arabia using Remotely Sensed Built Land Cover and Height Data. *Computers, Environment and Urban Systems*, Vol. 41, 167–176. https://doi.org/10.1016/j.compenvurbsys.2013.06.002.

[4] Resch, E., Bohne, R. A., Kvamsdal, T. and Lohne, J., (2016). Impact of Urban Density and Building Height on Energy Use in Cities. *Energy Procedia*, Vol. 96, 800–814. https://doi.org/10.1016/j.egypro.2016.09.142.

[5] Microsoft Bing Maps. Worldwide Building Footprints Derived from Satellite Imagery. *GitHub*. [Online]. Available: https://github.com/microsoft/GlobalMLBuildingFootprints#will-there-be-more-data-coming-for-other-geographies. [Accessed Jun. 10, 2024].

[6] Sirko, W., Kashubin, S., Ritter, M., Annkah, A., Bouchareb, Y. S. E., Dauphin, Y., Keysers, D., Neumann, M, Cisse, M. and Quinn, J. A., (2021). Continental-scale Building Detection from High Resolution Satellite Imagery. *ArXiv*, https://arxiv.org/abs/2107.12283.

[7] Li, X., Zhou, Y., Gong, P., Seto, K. C. and Clinton, N., (2020). Developing a Method to Estimate Building Height from Sentinel-1 Data. *Remote Sensing of Environment*, Vol. 240. https://doi.org/10.1016/j.rse.2020.111705.

[8] Li, M., Koks, E., Taubenböck, H. and van Vliet, J., (2020). Continental-scale Mapping and Analysis of 3d Building Structure. *Remote Sensing of Environment*, Vol. 245. https://doi.org/10.1016/j.rse.2020.111859.

[9] Frantz, D., Schug, F., Okujeni, A., Navacchi, C., Wagner, W., van der Linden, S. and Hostert, P., (2020). National-scale Mapping of Building Height Using Sentinel-1 and Sentinel-2 Time Series. *Remote Sensing of Environment*, Vol. 252. https://doi.org/10.1016/j.rse.2020.112128.

[10] Wu, B. W., Ma, J., Banzhaf, E., Meadows, M. E., Yu, Z. W., Guo, F., Sengupta, D., Cai, X. X. and Zhao, B., (2023). A First Chinese Building Height Estimate at 10 m Resolution (cnbh-10 m) Using Multi-Source Earth Observations and Machine Learning. *Remote Sensing of Environment*, Vol. 291. https://doi.org/10.10 16/j.rse.2023.113578.

[11] Bannakulpiphat, T. and Santitamnont, P., (2023) New Era of Mapping Products from UAV-based Oblique Camera System. *The 5th International Conference on Civil and Building Engineering Informatics*, 231-236

[12] Harmonized Sentinel-2 MSI: Multi Spectral Instrument Level 2A. *Google Earth Engine*. [Online]. Available: https://developers.google. com/earth-engine/datasets/catalog/COPERNIC US_S2_SR_HARMONIZED. [Accessed Feb. 20, 2024]

[13] Santitamnont, P., Research on Thai building modelling. *GitHub*. [Online]. Available: https://github.com/phisan-chula/Thai_Bldg_M odel. [Accessed Feb. 20, 2024].

[14] Huang, H., Chen, P., Xu, X., Liu, C., Wang, J., Liu, C., Clinton, N. and Gong, P., (2022). Estimating Building Height in China from ALOS AW3D30. *ISPRS Journal of Photogrammetry and Remote Sensing*. Vol. 185, 146–157. https://doi.org/10.1016/j.isprs jprs.2022.01.022.

[15] Ministerial Regulations Volume 33 (1992). Related with 1979 Thailand Building Control Act.